

Interdecadal variability of the overturning circulation in presence of eddy turbulence

Thierry.Huck@univ-brest.fr (LPO, Brest)

Florian.Sévellec@noc.soton.ac.uk (NOCS, Southampton)

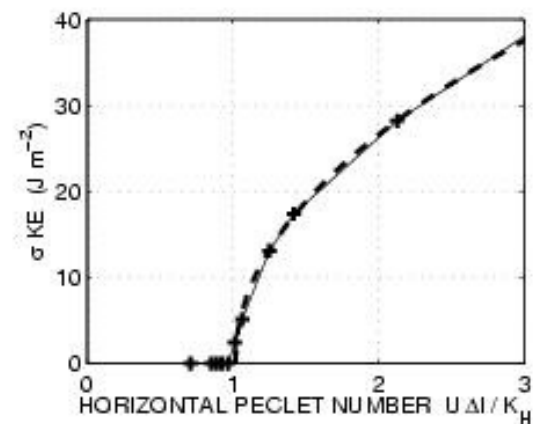
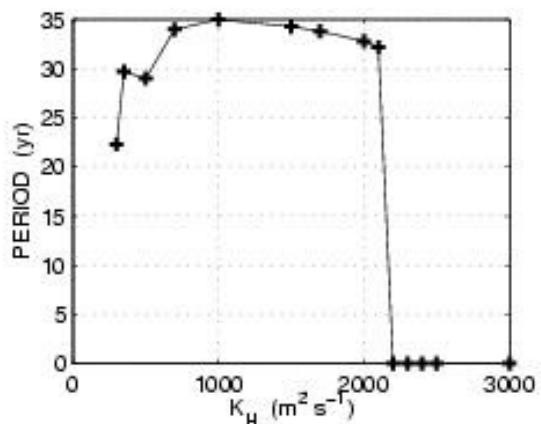
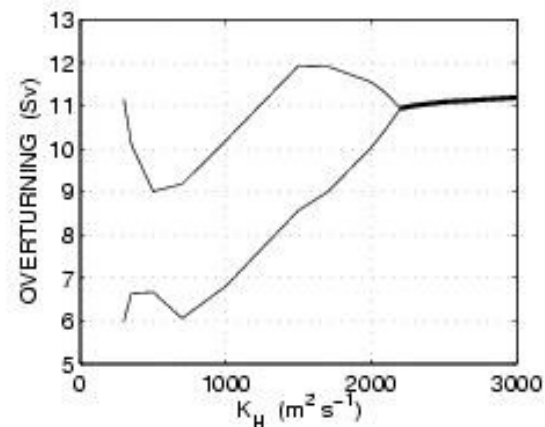
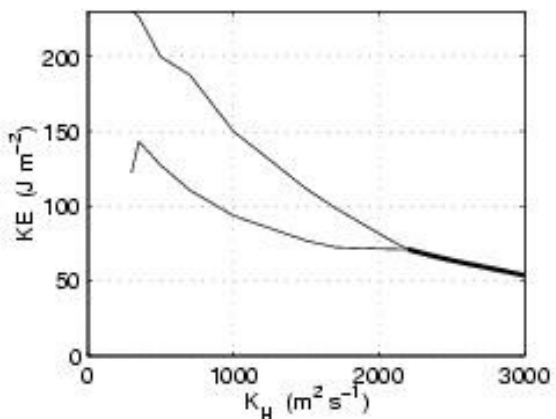
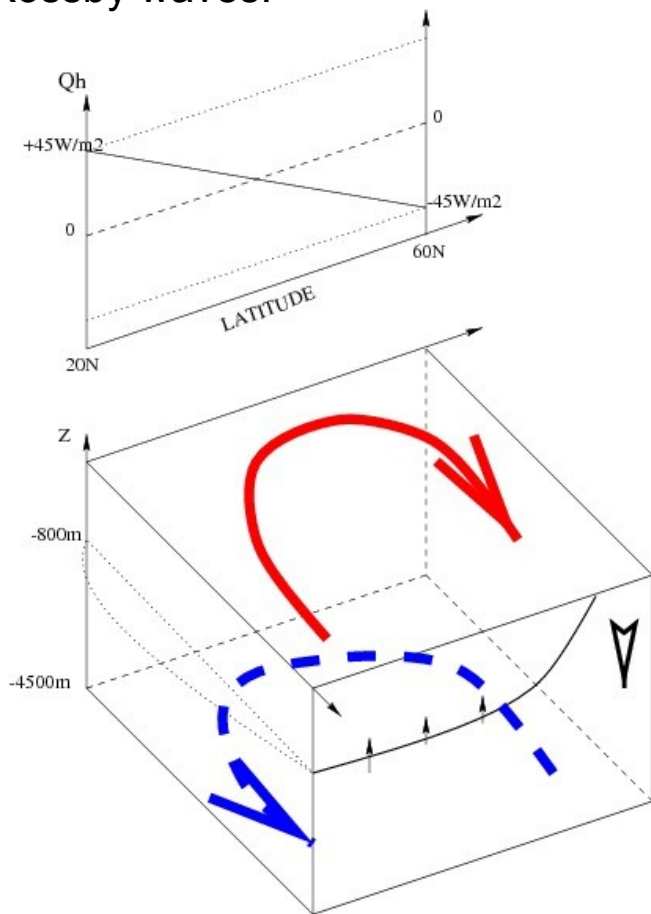
- A paradigm for the Atlantic Multidecadal Oscillation
- Influence of explicit eddy turbulence
- Influence of wind and eddy-driven variability
- More realistic model configurations (low resolution)

Contribution to Chaocean

- Methods of Linear Stability Analysis with OPATAM
- Application to mean state/seasonal cycle from various models
- Issues/questions

An overlooked paradigm for the low-frequency variability of the Overturning Circulation

Toy model: flat-bottom mid-latitude ocean basin, thermally forced only through surface heat flux, varying linearly with latitude. At low resolution $O(1^\circ)$, numerical integrations lead to steady states or multidecadal oscillations **depending on eddy diffusivity coefficient**. Mechanism: large-scale baroclinic instability, period $O(25\text{yr})$ associated with planetary Rossby waves.



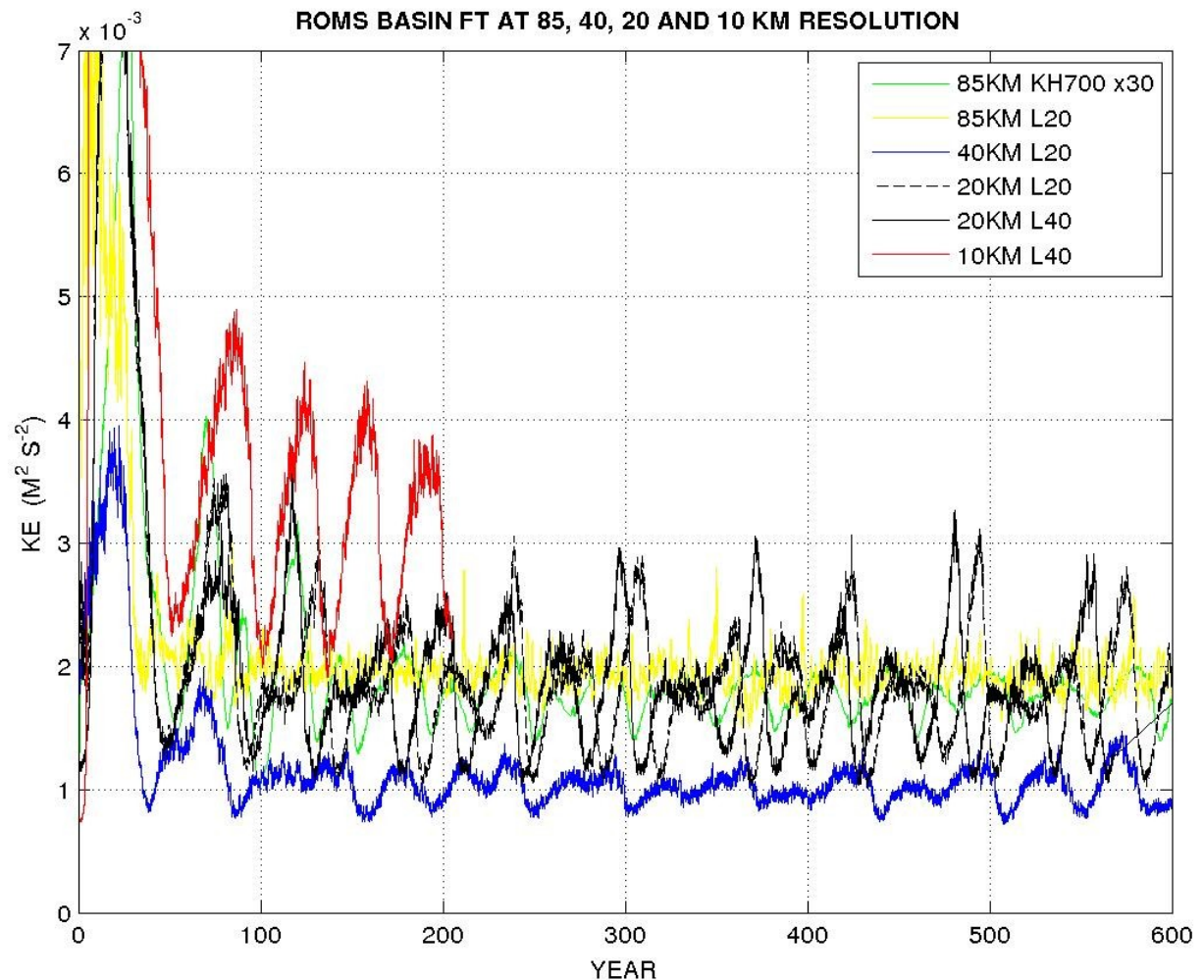
Bifurcation diagram as a function of the eddy diffusivity coefficient K_H . The oscillation period varies slightly around the bifurcation at $2200 \text{ m}^2/\text{s}$, the oscillations being damped (sustained) for a larger (weaker) diffusivity. The oscillation amplitude increases like the square root of the deviation from the critical coefficient. These two characteristics are typical of a **Hopf bifurcation**. Linear stability analysis show an unstable mode with growth time scale of 50 yr, ie extremely sensitive to surface restoring. (Huck & Vallis 2001 Tellus)

In what regime is a more realistic eddying ocean?

Same experiment (constant heat flux) conducted with ROMS at 85, 40, 20 and 10 km resolution, for 3 values of vertical mixing 10^{-4} , $3 \cdot 10^{-5}$ and $10^{-5} \text{ m}^2/\text{s}$.

The characteristics of the natural low-frequency variability of the thermohaline circulation vary significantly with the model resolution, that affects profoundly the mean circulation (no surprise), as well as the driving and damping mechanisms of the variability, the two interacting in both ways...

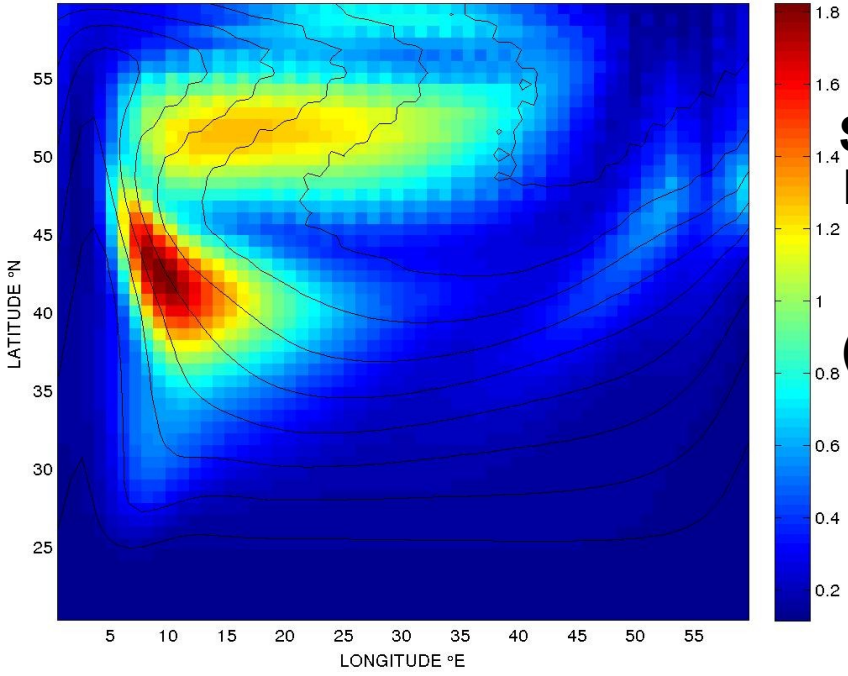
► **the decadal oscillations appear rather more robust to low vertical mixing with resolved eddies**



Total Kinetic Energy, although mostly Eddy KE, varies on decadal time scales with the mean ocean state.

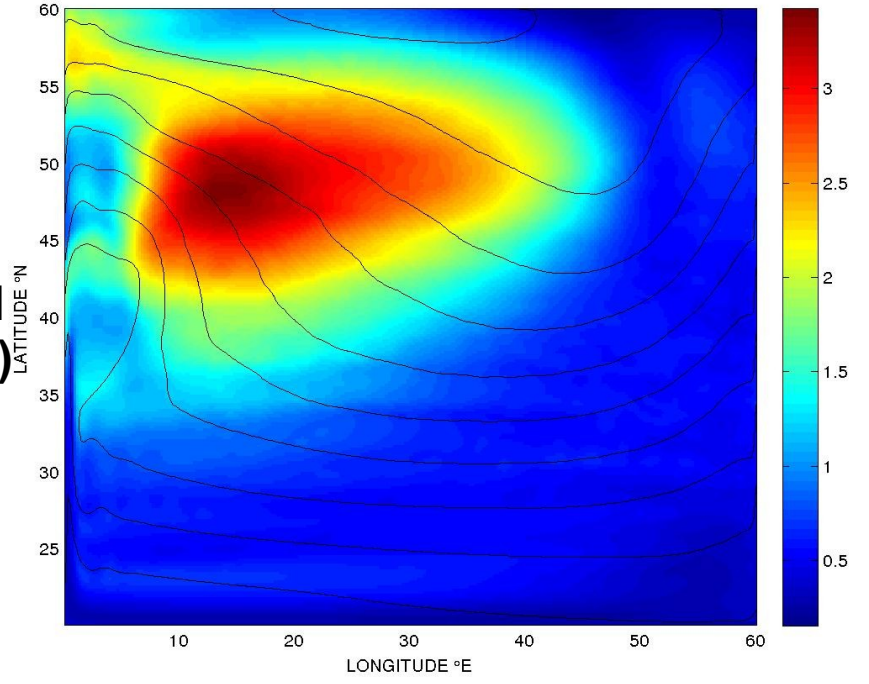
85 km

ROMS BASIN $K_V=1e-4$ YR=500-1000 SST 100 MEAN AND STD / °C mean=12.4119 std=0.41516



20 km

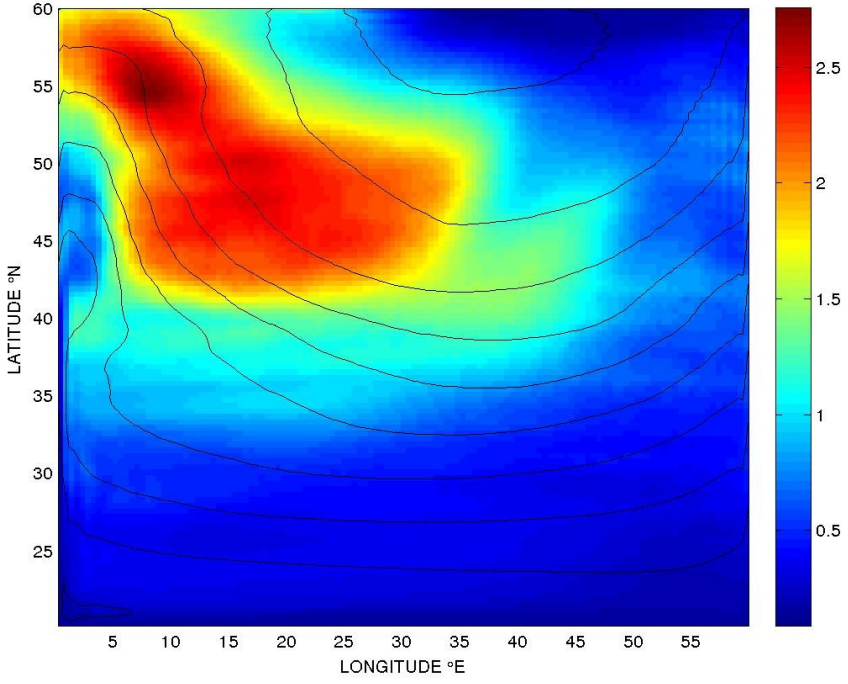
ROMS BASIN 20KM L40 $K_V=1e-4$ YR=821-1071 SST100 MEAN AND STD / °C mean=12.8687 std=1.1511



**SST
STANDARD
DEVIATION
(COLOR)
AND MEAN
(CONTOUR)
BASED
ON
ANNUAL
MEAN
FIELDS**

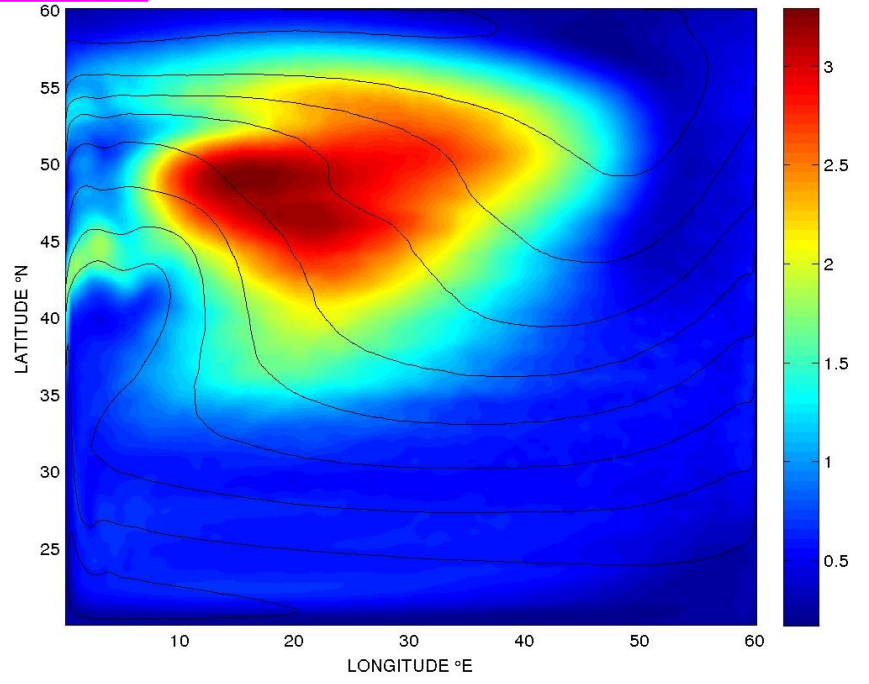
40 km

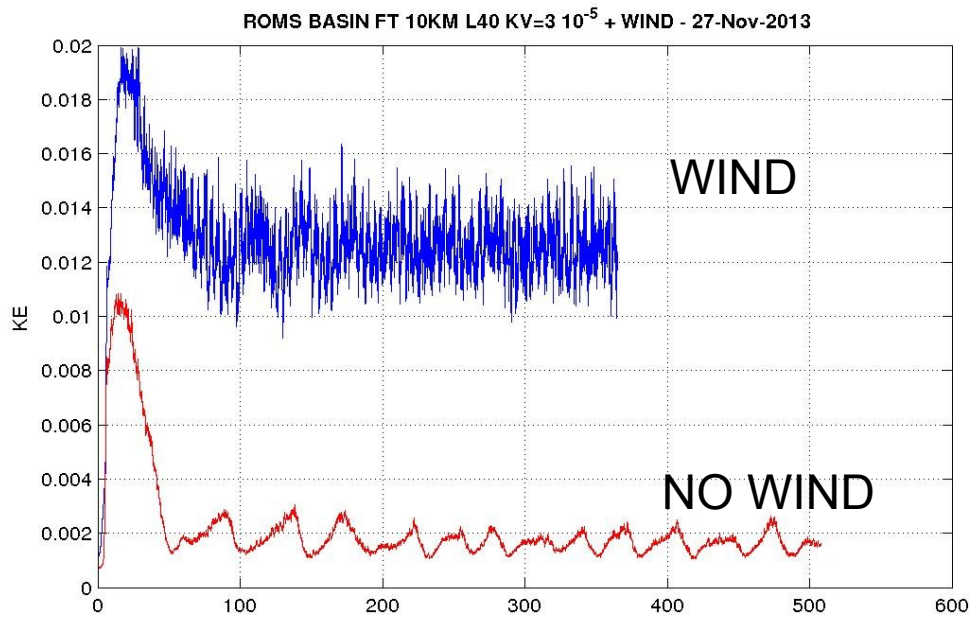
40KM $K_V=1e-4$ YR=2070-2270 SST100 MEAN AND STD / °C mean=12.2669 std=0.93877



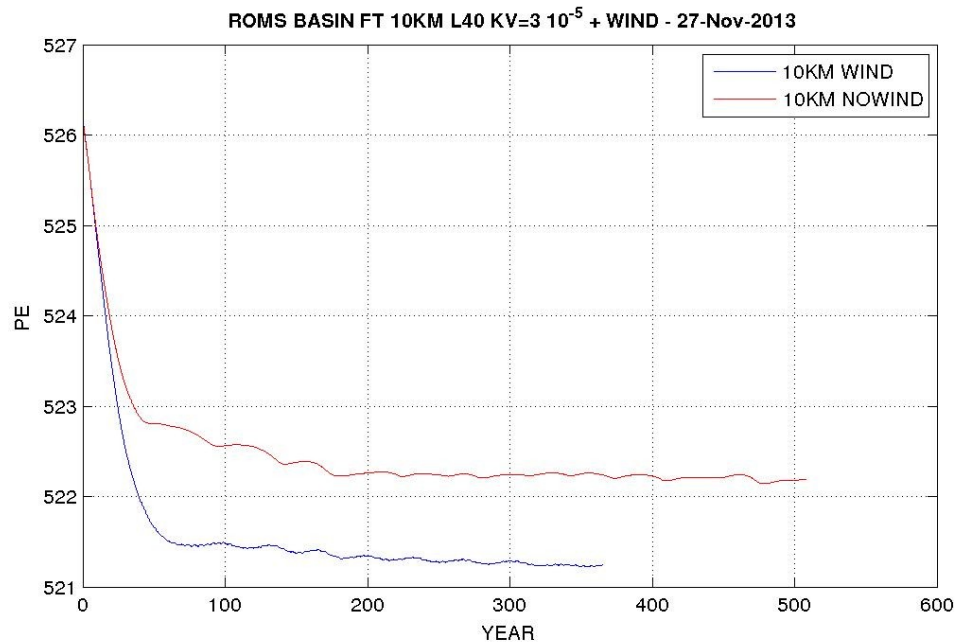
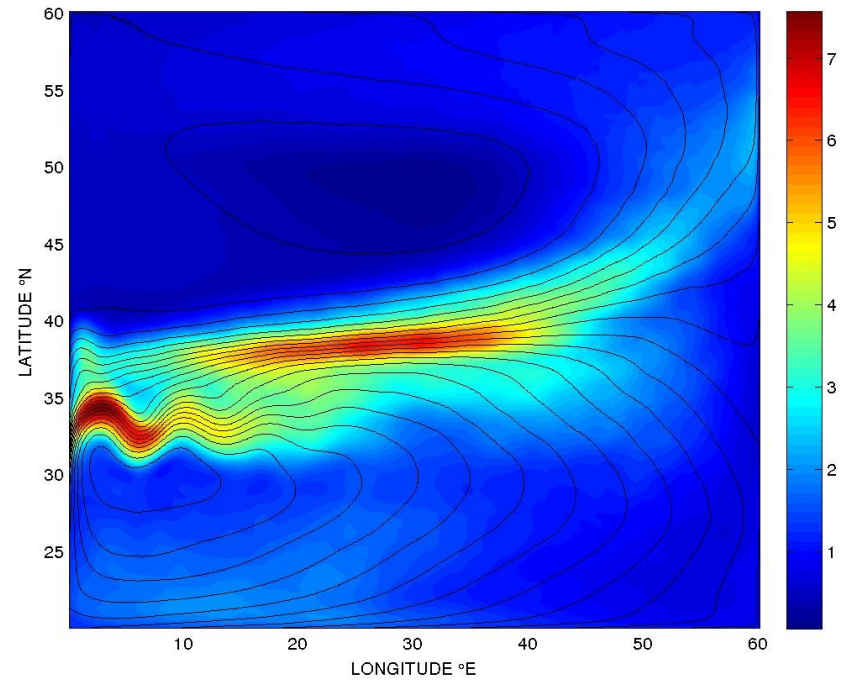
10 km

L40 $K_V=1e-4$ YR=288-514 SST100 MEAN AND STD / °C mean=12.9484 std=1.0562

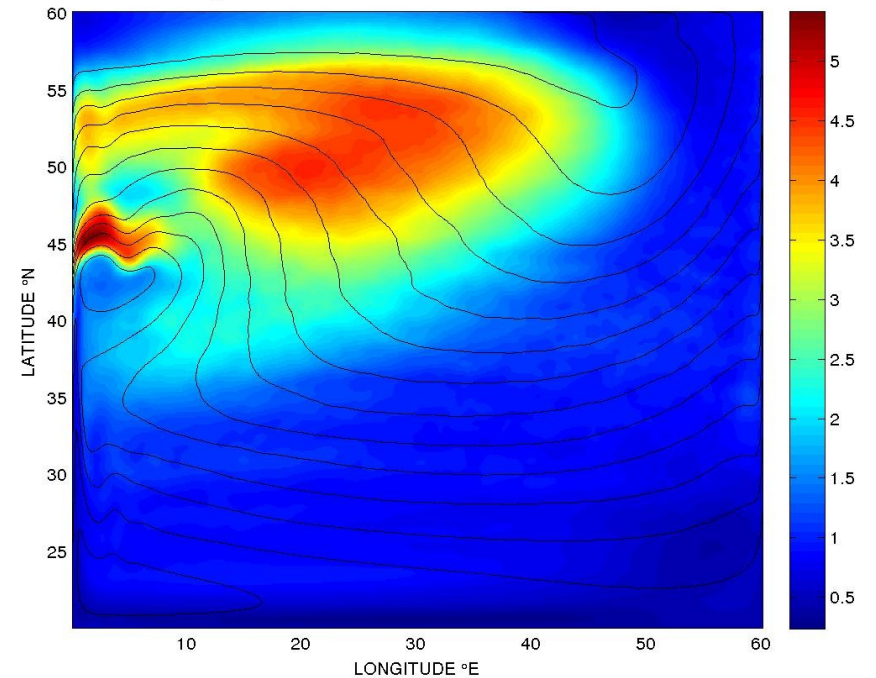




ROMS BASIN 10KM L40 $K_V=3e-5$ WIND YR=183-364 SST100 MEAN AND STD / °C mean=19.0935 std=1.5047



ROMS BASIN 10KM L40 $K_V=3e-5$ YR=253-507 SST100 MEAN AND STD / °C mean=18.6726 std=1.6847



► eddy-driven wind-induced variability has higher interannual frequency and pattern localized at the intergyre

Similar multidecadal oscillations in more realistic model configurations

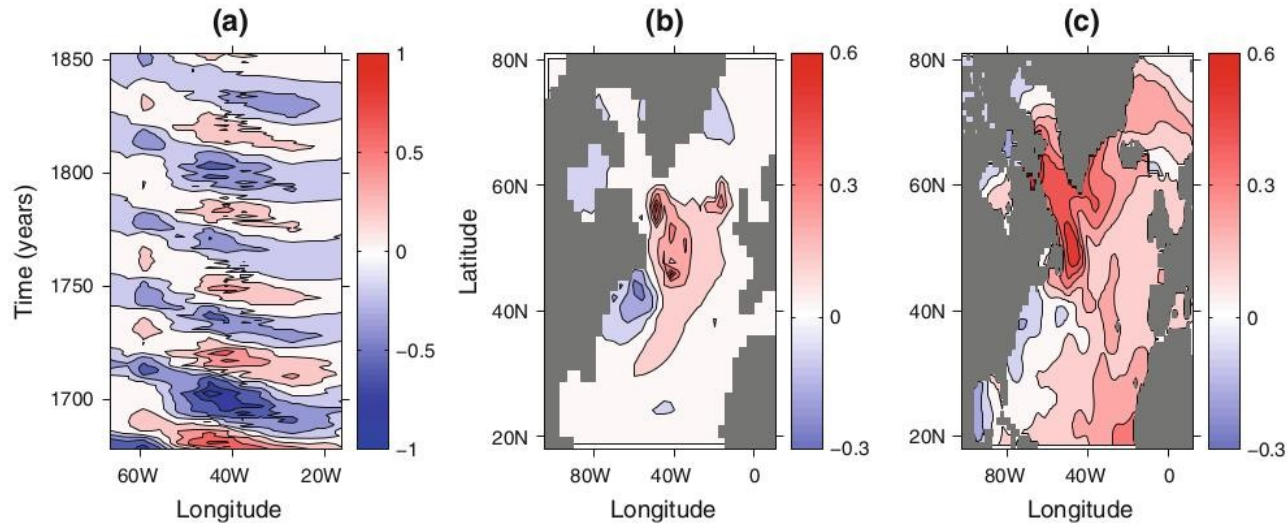


Fig. 14 Surface temperature pattern associated with the first interstadial phase (years 1650–1850) of the glacial experiment using an atmospheric CO_2 concentration of 190 ppm and a freshwater forcing of -0.21 Sv. **a** Characteristic $x-t$ diagram of meridionally averaged (43°N – 54°N) SST anomalies in the Atlantic basin. **b, c** SST

anomalies associated with one positive standard deviation of the AMO index, calculated by regression of surface temperatures with the index and multiplied by its standard deviation, similar to Knight et al. (2005), in the model (**b**) and in observations (**c**). See text for further details

UVIC intermediate complexity coupled model (Energy Moisture Balanced Atmosphere), around 3° resolution
► interdecadal oscillations during interstadials of millennial variability in a global coupled model (Arzel et al. 2012 CD)

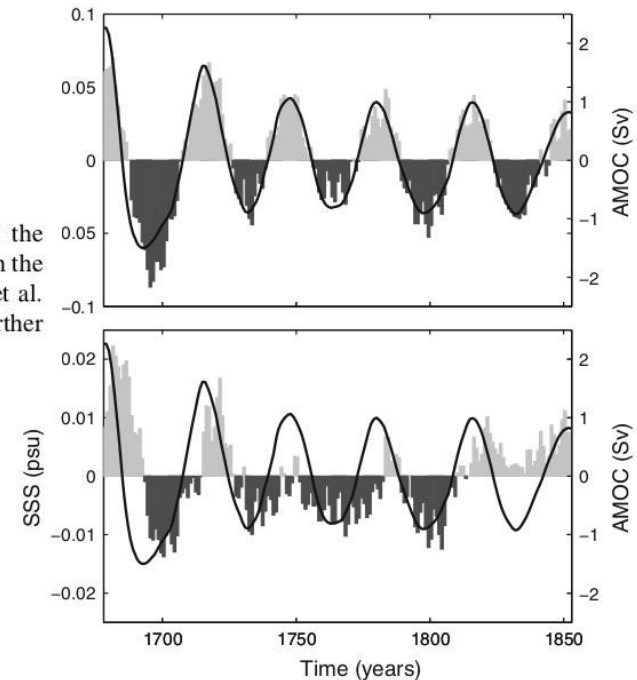


Fig. 11 Linearly detrended time series of maximum strength of the AMOC (black solid line), overlaid by detrended area weighted mean North Atlantic (0 – 70°N), **a** SST and **b** SSS annual mean anomalies during the first interstadial phase (years 1650–1850) of the glacial experiment using an atmospheric CO_2 concentration of 190 ppm and a freshwater forcing of -0.21 Sv (see Fig. 5). The AMO index corresponds to the SST timeseries in the *upper panel*

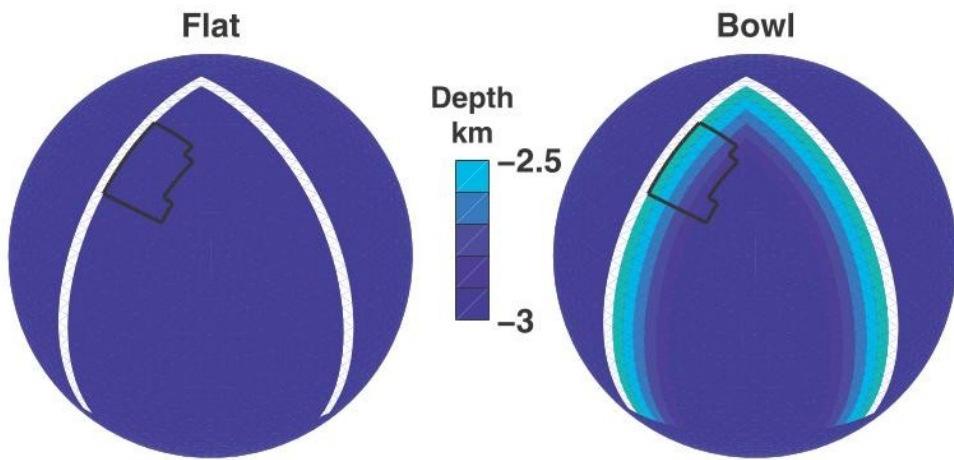


FIG. 1. Ocean geometry and depth (km) for (left) Flat and (right) Bowl. Two strips of land (white) extend from the north pole to 34°S, dividing the World Ocean into a small basin, a large basin, and a zonally unblocked southern ocean. In Flat In Bowl bathymetry is added to the small basin and t center of the basin to 2.5 km next to the meridional region along the western boundary of the subpolar boundary buoyancy (WBB) time series in section 3d.

MIT coupled model in idealized 2 basins configuration at low resolution $\sim 4^\circ$: multidecadal oscillation sensitive to topography (Buckley et al. 2012 JCLim)

► PhD research of Quentin Jamet in Brest : sensitivity of these oscillations to horizontal resolution. At 2° and 1° , oscillations are robust, with more complex MOC variability pattern at 1°

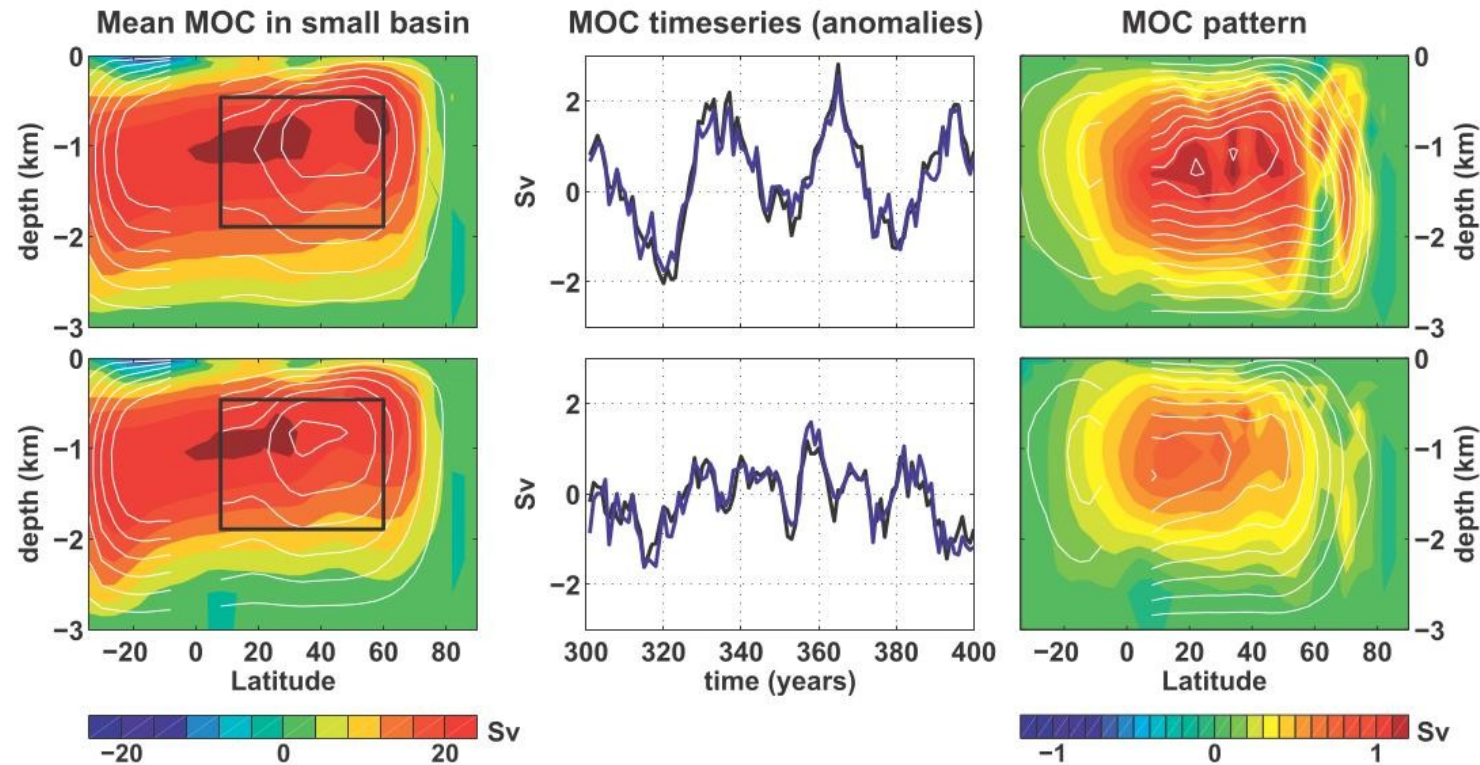
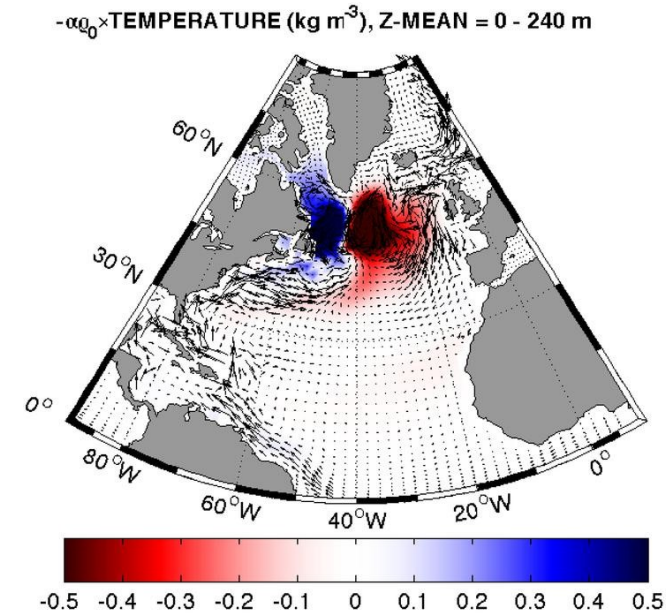
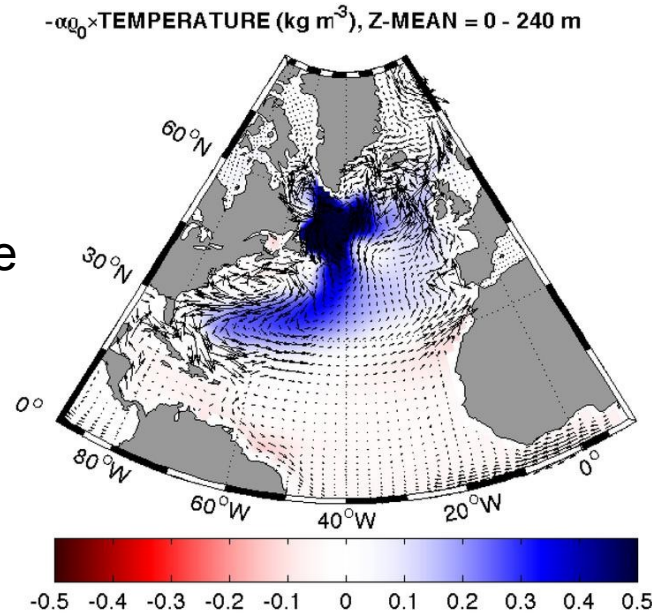


FIG. 3. (left) The residual mean MOC in the small basin (colors) and the MOC diagnosed from Eq. (5) (black/white contours) for (top) Flat and (bottom) Bowl. White (black) contours correspond to a positive (negative) MOC and the contour interval for both colors and black/white contours is 4 Sv. The black box shows the latitude and depth range (8° – 60° N, 460–1890-m depth) used to define the MOC time series. (middle) A 100-yr segment of anomalies of the yearly MOC time series (black) and reconstructed MOC time series [diagnosed from Eq. (5), blue] for (top) Flat and (bottom) Bowl. (right) The spatial patterns of MOC variability obtained by projecting MOC anomalies onto the MOC index (colors) and projecting MOC anomalies diagnosed from Eq. (5) onto the reconstructed MOC index (black/white contours) for (top) Flat and (bottom) Bowl. White (black) contours correspond to positive (negative) MOC anomalies and the contour interval for both the colors and black/white contours is 0.1 Sv.

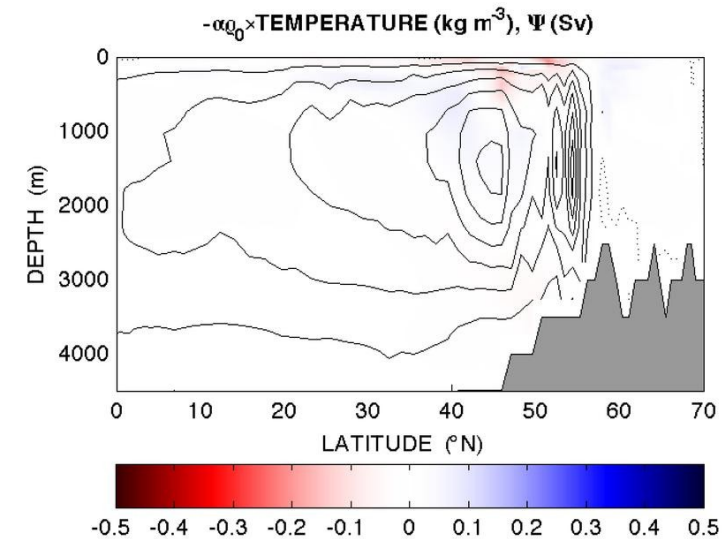
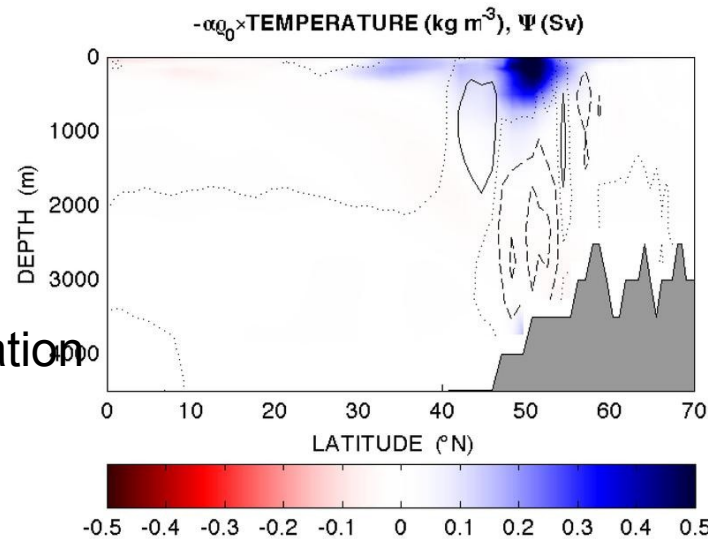
OPA ORCA2° model configuration + OPATAM (Sévellec&Fedorov 2013)

Anomalies of upper-ocean temperature (0-240m) and surface currents. Temperature is given in terms of density.



Anomalies of meridional streamfunction and zonally averaged temperature.

for 2 phases of the oscillation
Amplitude is arbitrary
(linear mode).



Spatial structure of the least-damped eigenmode of the tangent linear model: (left) a large temperature anomaly spreads over the northern Atlantic, but the AMOC anomaly is close to zero; (right) it evolves 6 yr later into a dipole-like anomaly, associated with a strong AMOC.

Contribution to Chaocean: from ORCA2 to ORCA12...

Development/use of several tools from dynamical system theory:

- linear stability analysis, allowing to forecast growing modes of variability, but also more interestingly damped modes that can develop under some excitation (atmospheric or eddies)
- "empirical" LSA (Sévellec&Fedorov 2013), far more efficient
- optimal perturbations (Sévellec et al. 2008 JPO)

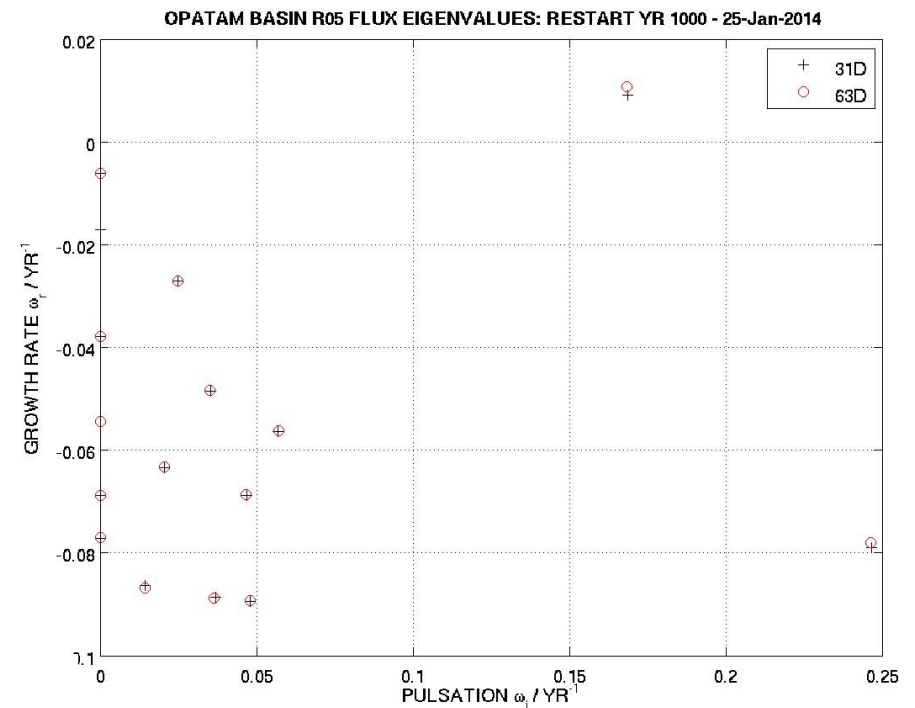
All are based on tangent linear and/or adjoint model integration (OPATAM... NEMOTAM), for now in ORCA2° or simpler configs.

Plan to use some of these methods to find leading modes on various models mean state/seasonal cycle:

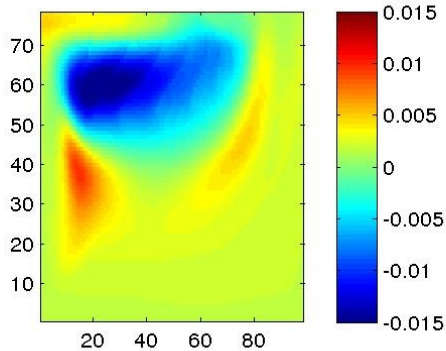
- link between model variability and leading eigenmodes?

Linear Stability Analysis with OPATAM+ARPACK

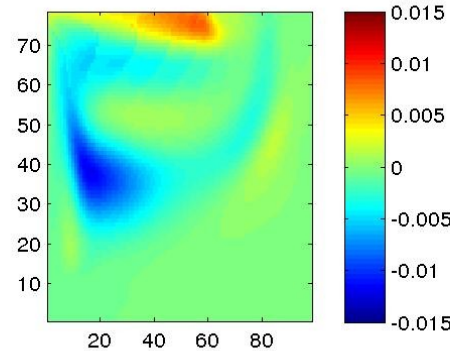
leading eigenvalues spectrum →
one unstable mode, period 37yr
growth time scale 109yr



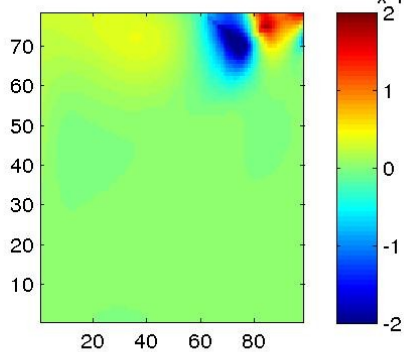
OPATAM BASIN R05 FLUX: MODE 1 REAL $k=1$



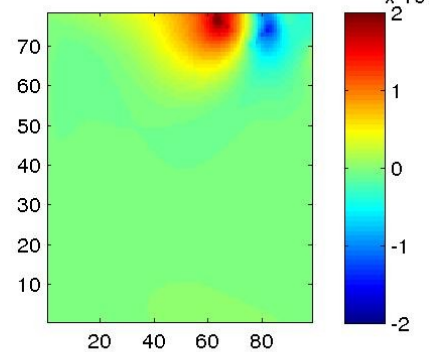
MODE 2 IMAG $k=1$



OPATAM BASIN R05 FLUX: MODE 1 REAL $k=10^{-3}$



MODE 2 IMAG $k=10$



/home/thuck/opatam/basin

► full LSA of an idealized basin configuration of OPA, reproducing with a much more complex and versatile tool results obtained in Planetary Geostrophic dynamics 12 yr ago (Huck&Vallis 2001 Tellus)

► now at $1/2^\circ$ resolution to test timing & methods before moving to ORCA2 realistic configuration

Issues

With increasing model resolution,

- large-scale instabilities usually grow/decay slowly $O(1-100 \text{ yr})$

- mesoscale instabilities grow fast $O(20\text{d})$ on scales $n \times R_d$

a linearized model with eddy-resolving parameters may only see the latter.

Two approaches:

- remain at low-resolution and parameterize the eddies,

- use eddy-resolving models but filter the scales of the perturbations for LSA.

Practical issues now

- project/interpolate HR model outputs on LR model grid... (not tested yet because of annual-cycle trajectory necessary for the tangent model)

- use robust-diagnostic LR simulation to hopefully match HR state? (usually difficult to be satisfied with both tracer and velocity fields...)

presently using seasonal cycle with strong $O(30-60\text{d})$ 3D restoring decaying/depth.

- perform analysis on high-resolution model with some filter on the scale (NEMOTAM parallelized) : to be tested in a shallow-water model soon

Conclusions

- ▶ Processes generating intrinsic Low-Frequency Oceanic Variability: can we distinguish eddy-driven vs large-scale processes?
- ▶ It is still a rather overlooked aspect of the large-scale thermohaline circulation that it develops intrinsic low-frequency variability when forced by prescribed fluxes of buoyancy instead of restoring surface properties (more appropriate for the largest scales). **We believe it is a generic property, just like the wind-eddy-driven variability, as soon as the amplitude of the overturning is large enough and/or the damping through diffusivity/viscosity low enough.** But it results from a linear unstable mode of the large scale circulation...
- ▶ how sensitive are least damped modes to mean circulation, model resolution, sub-grid-scale parameterizations, seasonal cycle ?

file:///Users/thuck/Desktop/EGU2013/movie_sst100_40km.avi

Animation of Sea Surface Temperature (0-100m), annual means, for different resolution simulations.

References cited

Arzel, O., M. H. England, A. Colin de Verdière, and T. Huck, 2012: Abrupt millennial variability and interdecadal-interstadial oscillations in a global coupled model: sensitivity to the background climate state. *Clim. Dyn.*, 39, 259-275.*

Buckley, M. W., D. Ferreira, J.-M. Campin, J. Marshall, and R. Tulloch, 2012: On the relationship between decadal buoyancy anomalies and variability of the Atlantic meridional overturning circulation. *J. Clim.*, 25, 8009-8030.

Huck, T., G. K. Vallis, and A. Colin de Verdière, 2001: On the robustness of the interdecadal modes of the thermohaline circulation. *J. Clim.*, 14, 940-963.*

Huck, T., and G. K. Vallis, 2001: Linear stability analysis of the three-dimensional thermally-driven ocean circulation: application to interdecadal oscillations. *Tellus*, 53A, 526-545.*

Greatbatch, R. J., and S. Zhang, 1995: An interdecadal oscillation in an idealized ocean basin forced by constant heat flux. *J. Clim.*, 8, 81-91.

Sévellec, F., T. Huck, M. Ben Jelloul, N. Grima, J. Vialard, and A. Weaver, 2008: Optimal surface salinity perturbations of the meridional overturning and heat transport in a global ocean general circulation model. *J. Phys. Oceanogr.*, 38, (12) 2739-2754,*

Sévellec, F., A. V. Fedorov, 2013: The leading, interdecadal eigenmode of the Atlantic meridional overturning circulation in a realistic ocean model. *J. Clim.*, 26, 2160-2183.

de Raaf, L. A., and H. A. Dijkstra, 2002: Instability of the thermohaline ocean circulation on interdecadal time scales. *JPO*, 32, 138-160.

*available on my website <http://www.ifremer.fr/lpo/thuck/publis/publications.html>